# A Hybrid Parallel Robot

Huapeng Wu , Pekka Pessi, Heikki Handroos
Lappeenranta university of Technology
Association Euratom-Tekes, Filand
Email: huapeng@lut.fi

***Abstract*—This paper presents a novel mobile parallel robot carries out welding and machining processes in assembly and repair of vacuum vessel (VV) of reactor (ITER). The kinematics of the robot has been optimized for the ITER's access. The kinematics analysis of the robot construction is given in the paper and the welding and machining experiments are demonstrated by a limited prototype.**

***Keywords*—ITER, parallel robot, laser welding, cutting**

## I. INTRODUCTION

The ITER sectors require more stringent tolerances, ±5mm, than normally expected for the size of structure involved. The walls of ITER sectors are made of 60mm-thick stainless steel and are joined together by the high efficiency structural and leak tight welds. In addition to the initial vacuum vessel assembly, the sectors may have to be replaced for repair. Parallel robot has high stiffness, high dynamic performance, and good payload to weight ratio in comparison with the conventional serial robots [1] [4] [5], and suitable for the task.

For the assembly of the ITER vacuum vessel sector, the precise positioning of welding end-effectors, at some distance in a confined space from the available supports, will be required, which is not possible using conventional machines or robots. In this paper, a special parallel robot is presented, which is able to carry out welding and machining processes from inside of the ITER vacuum vessel. It consists of a ten-degree freedom parallel mechanism mounted on a carriage driven by electric motor/gearbox on a rack. The robot carries: (1) welding gun, such as a TIG, hybrid laser or e-beam welding gun, to weld the inner and outer walls of the ITER vacuum vessel sectors; and (2) machining tools to cut and milling the walls with necessary accuracy. It can carry other tools and material to a required position inside the vacuum vessel.

The robot offers not only a device but also a methodology for the assembling and repairing of VV. For assembling, an on-line six-degree freedom seam finding algorithm has been developed, which enables the robot to find welding seam automatically in a very complex environment. In machining, the multi-flexible machining method carried out automatically by the robot has also been investigated, which includes edge cutting, smoothing, and defect point milling. The kinematic design of the robot has been optimized for the ITER access and a hydraulically actuated pre-prototype has been built. Finally the experimental results are presented and discussed. The earlier development phases of the robot are presented in [2] and [3].

## II. STRUCTURE OF VV AND ASSEMBLY PROCESS

The inner and outer walls of the ITER Vacuum Vessel (VV) are made of the 60mm-thick stainless steel, 316L, and are welded together indirectly with an intermediate so-called "splice plate" inserted between the sectors to be joined. This splice plate has two important functions: to allow access to bolt together the thermal shields between the VV and coils, and to compensate for the mismatch between the adjacent sectors to give a good fit-up of the sector-sector butt weld. The robot end-effector will have to pass through the inner wall splice plate opening to reach the outer wall. As shown in Fig.1, the assembly process has to be carried out from inside of the vacuum vessel. The assembly or repair will be performed according to four phases: cutting, edge machining and smoothing, welding, and NDT control. The robot acts as a transport device for welding, machining, and inspection. The maximum robot force arises from cutting, and the dynamic force can be up to 3KN.

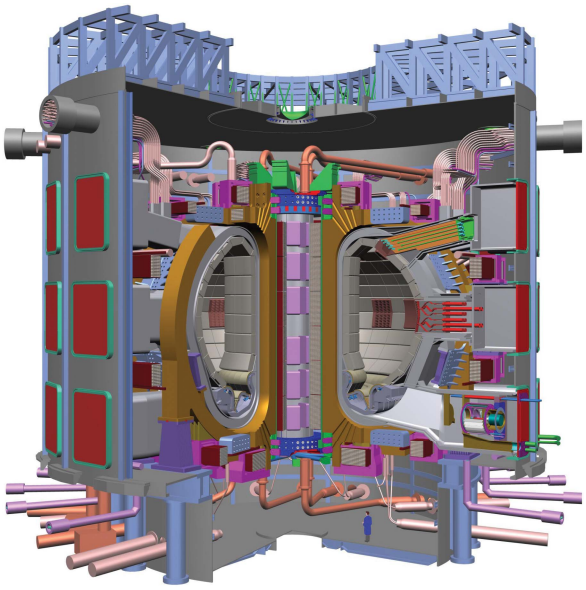

Figure 1. ITER

978-1-4244-1676-9/08 /$25.00 ©2008 IEEE

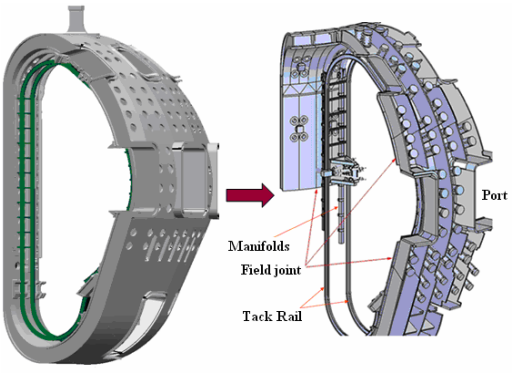


Figure 2. Track rail fixed inside VV

To operate in the cross section of the vessel, a track, with a rack on one side of the rail supported by manifolds and beams, is assembled inside the sector (Fig.2).

The robot driven on the rail carries out welding or machining along the edge of the sector. After finishing the assembly of two sectors, the robot moves to the next sector with a track assembled. After finishing the last sector assembly, the robot can be taken out via the port of VV.

## III. PARRLLEL ROBOT AND KINEMATICAL MODEL

### A. *Structure of robot*

The new parallel robot has ten-degree freedom proposed by H. Wu (Fig.3), and consists of two relatively independent sub-structures: (i) Hexa-WH — a Stewart platform-based parallel mechanism driven by six water hydraulic cylinders contributing full six-degree freedom for the end-effector; and (ii) carriage, which offers Hexa-WH four-degree freedom, i.e., tip motion, rotation, linear motion, and tracking motion, to enlarge the workspace and to offer the high mobility of robot. It is a hybrid redundant manipulator since it has extra four-degree freedom provided by carriage. The carriage mainly consists of 6 units:

*1) Carriage frame:* The carriage frame is a complex structure welded by multi-steel-plates, and it is able to carry high payload and offer enough room to maintain mechanisms. The stiffness and weight are the most important indexes in the design and it has been optimized to achieve necessary stiffness with light weight.

*2) Tracking drive unit:* The tracking drive unit consists of electric motor, reduction unit CYCLO, V-shape bearing, and driving gear. The electric servo motor with position feedback controller offers high accurate motion. In order to output great torque needed to drive great mass and payload, the reduction unit CYCLO is added to the motor to reduce speed and transmit high torque to the drive gear. Two V-shape wheels keep the carriage on the tracking rail at right position to avoid cross motion. Two drive units are used in the carriage to offer enough torque to drive the robot and payload inside VV.

*3) Compensation mechanism:* The compensation system is an important unit that limits the backlash caused by inaccurate assembling of tracking rail and compensates distance changing between the wheels in bending area.

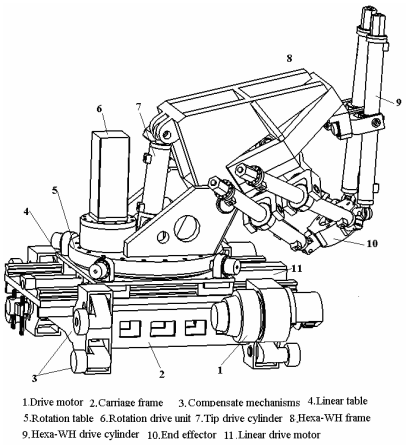


Figure 3. Parallel robot

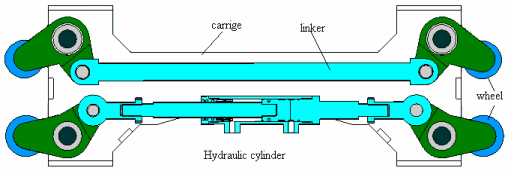


Figure 4. Compensation mechanism

As the shape of VV is very complicated, it is very difficult to keep the tracking rails lying on the VV surface in accurate position. The position tolerance can be up to ±2mm. The distance of couple wheels is changed in bending area. During motion all wheels must touch the parallel rails with certain force, thus an adaptive distance compensation system is needed. The compensation system should be able to take the summed weight of robot and payload, when robot is upside down at the top position inside VV. Since the total payload is very heavy, a hydraulic cylinder is applied to justify the compensation force according to the position where the robot is located. Fig. 4 shows the compensation system, where the upside is the tolerance adaptive mechanism and the downside is the hydraulic distance compensation system.

*4) Linear drive unit:* The linear drive unit enlarges the workspace of robot, and consists of five parts: ball screw drive unit, servo motor, rails, linear bearings, and a table. Two parallel rails are fixed on the carriage frame to offer motion crossing the frame and to extend the distance of robot in Y direction. In this direction the difference of one VV sector from the inner board to the outer board can be 900mm, i.e., the robot needs longer reach than in other directions. The linear drive unit helps the robot end-effector to reach the farther border of the VV.

*a) Rotation drive unit:* The rotation drive unit offers a rotation motion along the Z axe so that the robot can machine the flex houses on the inner wall at any position. The rotation

drive unit consists of slewing bearing, drive gear, reduction unit CYCLO, and servo motor.

*b) The slewing bearing:* Integrates bearing and gear together, leading to a compact structure with light weight. The rotation of the unit can reach ±180°.

*5) Tip drive unit:* The tip drive unit, being driven by one servo control hydraulic cylinder, offers one more rotation to Hexa-WH.

*6) Hexa-WH:* A Stewart based mechanism, driven by six servo control water hydraulic cylinders, offers six-degree freedom to the end-effector, where the machining head and welding gun are mounted. Because of the special shape of VV, a full six-degree freedom motion for tool is needed to enable the robot to carry out welding and machining. Hexa-WH can offer the required accuracy and the high force capacity due to its novel configuration and the hydraulic drive.

*B. Kinematics model*

*1) Forward kinematics*: As described above, the carriage offers the robot the four-degree freedom - two linear motions and two rotations, and the Hexa-WH offers the end-effector the full six-degree freedom. The transformation matrix of the robot can be defined as:

$$T_c = T_1 \cdot T_2 \cdot T_3 \cdot T_4 \cdot T_5 \tag{1}$$

Where

$$T_1 = \begin{bmatrix} 1 & 0 & 0 & X_1 \\ 0 & 1 & 0 & Y_1 \\ 0 & 0 & 1 & Z_1 \\ 0 & 0 & 0 & 1 \end{bmatrix},$$

$$T_2 = \begin{bmatrix} 1 & 0 & 0 & X_2 \\ 0 & 1 & 0 & Y_2 \\ 0 & 0 & 1 & Z_2 \\ 0 & 0 & 0 & 1 \end{bmatrix},$$

$$T_3 = \begin{bmatrix} c\phi & -s\phi & 0 & X_3 \\ s\phi & c\phi & 0 & Y_3 \\ 0 & 0 & 1 & Z_3 \\ 0 & 0 & 0 & 1 \end{bmatrix},$$

$$T_4 = \begin{bmatrix} 1 & 0 & 0 & X_4 \\ 0 & c\varphi & -s\varphi & Y_4 \\ 0 & s\varphi & c\varphi & Z_4 \\ 0 & 0 & 0 & 1 \end{bmatrix},$$

$$T_5 = \begin{bmatrix} c\alpha c\beta & c\alpha s\beta s\gamma - s\alpha c\gamma & c\alpha s\beta c\gamma + s\alpha s\gamma & X_5 \\ s\alpha c\beta & s\alpha s\beta s\gamma + c\alpha c\gamma & s\alpha s\beta c\gamma - c\alpha s\gamma & Y_5 \\ -s\beta & c\beta s\gamma & c\beta c\gamma & Z_5 \\ 0 & 0 & 0 & 1 \end{bmatrix}.$$

Once the parameters of joints are given, the forward kinematics of the robot can be defined as

$$\vec{P} = T \bullet \vec{P}_0 = T_1 \cdot T_2 \cdot T_3 \cdot T_4 \cdot T_5 \cdot \vec{P}_0 \cdot \tag{2}$$

To solve the forward kinematic model of the Hexa-WH, the numeric iterative method can be employed.

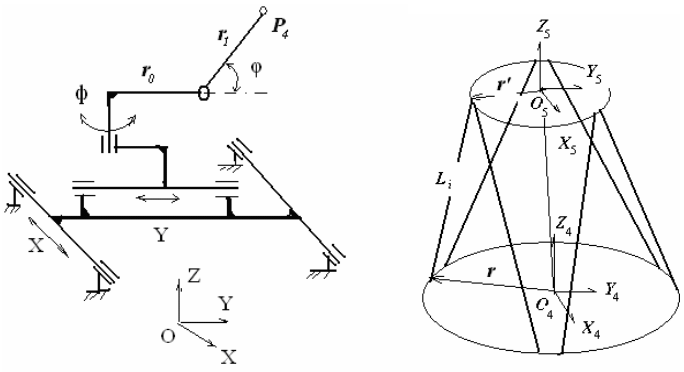


Figure 5. Mechanism of carriage and Hexa-WH

*2) Inverse kinematic model of robot:* As the robot has four-degree freedom redundancies, we can give an inverse kinematic model to first the carriage, then to the Hexa-WH.

*a) Inverse kinematic model of carriage:* The inverse kinematic model of carriage is defined to find the values of the four actuators with respect to the frame o for a given position and an orientation of P4 on the Hexa-frame. The principle of the carriage mechanism is shown in Fig. 5 of left side. In the application, rotation angle $\phi$ is fixed only at a few values, 0°, ±90°, and 180°, and we can calculate the values of other actuators by fixing $\phi$, i.e., for a given position $P_4$(x, y, z), the centre of the Hexa-Frame, we have

$$X + (r_0 + r_1 \cos\varphi)\cos\phi = x \tag{3}$$

$$Y + (r_0 + r_1 \cos\varphi)\sin\phi = y \tag{4}$$

$$r_1 \sin\varphi = Z \tag{5}$$

Then

$$\varphi = \arcsin(Z / r_1) \tag{6}$$

$$X = x - (r_0 + r_1 \cos\varphi)\cos\phi \tag{7}$$

$$Y = y - (r_0 + r_1 \cos\varphi)\sin\phi \tag{8}$$

*b) Inverse kinematic model of Hexa-WH:* The inverse kinematic model for the Hexa-WH is defined to find the values for each cylinder at a given position and an orientation of the end-effector with respect to the Hexa-frame. Here $O_4$ is coincided with $P_4$ on the carriage side. Fig.5 of right side demonstrates the coordinates of the Hexa-WH. The inverse kinematic model for the Hexa-WH is

$$\vec{L}_i = \overrightarrow{O_4O_5} + R \cdot \vec{r}_i' - \vec{r}_i \ (i = 1, 2, \ldots, 6), \tag{9}$$

where

$$R = \begin{bmatrix} c\alpha c\beta & c\alpha s\beta s\gamma - s\alpha c\gamma & c\alpha s\beta c\gamma + s\alpha s\gamma \\ s\alpha c\beta & s\alpha s\beta s\gamma + c\alpha c\gamma & s\alpha s\beta c\gamma - c\alpha s\gamma \\ -s\beta & c\beta s\gamma & c\beta c\gamma \end{bmatrix}$$

where $\vec{r}_i$ is the vector of the joint of the i[th] cylinder on the Hexa-frame with respect to frame o4 and $\vec{r}_i'$ is the vector of the joint of the i[th] cylinder on the end-effector with respect to frame $O_5$.

The length of each cylinder can be found, when (x, y, z, $\alpha$ , $\beta$ , $\gamma$ ) is defined with respect to frame o4

$$l_i = \left|\vec{L}_i\right| = \sqrt{(\overrightarrow{O_4O_5} + R\cdot\vec{r}_i' - \vec{r}_i)\bullet(\overrightarrow{O_4O_5} + R\cdot\vec{r}_i' - \vec{r}_i)} \qquad (10)$$

There are two ways to combine the two inverse kinematic models to get the solution of the whole robot. One simple way is to calculate the coordinates (x, y, z, $\alpha$ , $\beta$ , $\gamma$ ) of the end-effector with respect to $\{O_4\}$ and the values for each actuator from equations (3-10) for the given coordinates of the end-effector with respect to frame {o}, while fixing $\{O_4\}$ at a certain position with respect to frame {o} according to experience. The other way is to use an optimization algorithm to find redundant solution, which is subjected to minimize the deflection of the robot during motion, i.e., $\min_{\bar{l}} f(\bar{q},\bar{l})$, where f is the deflection model of the robot, $\bar{q}$ is the position vector of the end-effector, and $\bar{l}$ is the value vector of ten actuators. For a given $\bar{q}$ we can find $\bar{l}$ by solving the optimization problem $\min_{\bar{l}} f(\bar{q},\bar{l})$.

## IV. Hardware and Software

Because there are no commercial controller and software available for the special functions of the parallel robot, an open architecture of hardware and programmable software are being developed. Fig.6 shows the structure of hardware control system. The controller is an industrial-PC-based motion controller. It provides a reliable and easy-at-use environment for controlling the robot because Ethernet bus is used in the connection of iPC and I/O interfaces.

The software is defined in Fig.7, including graphical interface, trajectory planning, forward and inverse kinematics models, interpolator, controller, and I/O interface functions. And those functions have to be integrated with the program offered by iPC and run completely in real time.

- Graphical interface is a high level program, it includes parameter setting, condition monitoring, and graphical visualization functions. User can easily exchange information with this program.
- Trajectory planning is also a high level program. As the robot has redundant actuators, the trajectory planning is much more difficult than usual, so an optimization algorithm, which is subjected to minimize the deflection of the robot during motion, has been employed.
- Forward and inverse kinematics models and interpolator are real time functions, which generate data for motion controller.

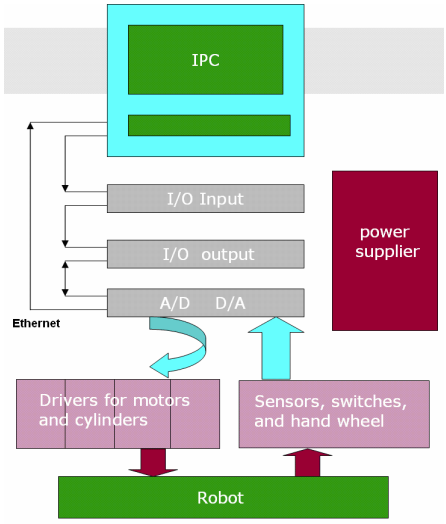


Figure 6. Structure of robot controller

- Controller is a real time function including water hydraulic controller and motor controller. As the robot has two tracking motors and the speed of the motors are not always the same at some positions, a master–slave control algorithm has been used.
- I/O interface functions are real time functions, which enable transferring date from sensor to controller and from controller to driver.

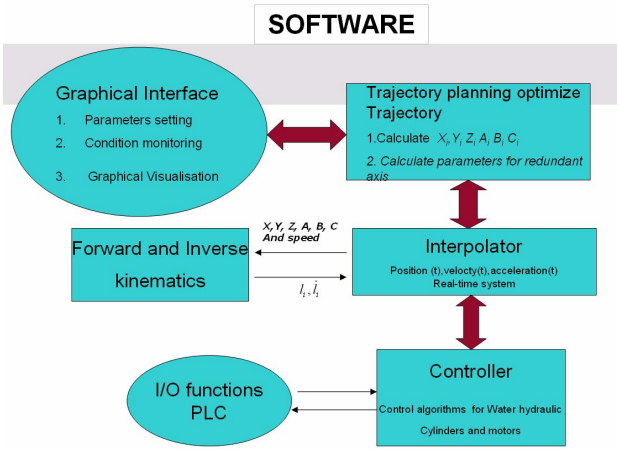


Figure 7. Structure of software

## V. Machining and Welding Test Mock-up

Fig.8 shows the experiment setup for testing the cutting, welding with VVPSM. First the robot carries the cutting tool to cut VVPSM into two parts, then a splice plate is inserted into the gap between the separate parts, following this, by using the narrow gap TIG welding and Laser welding, the splice plate are jointed to the separate parts of VVPSM. In ITER assembly, the high quality welds are required to avoid the leak of tritium. To guarantee the welding quality, a seam tracker, which guides the robot motions along the centre of the welding seam, is employed. A scout seam tracker used in the experiments is the six-degree freedom seam finder, is made by Dr.Barthel Sensor

system GmbH. It offers 6 DOF local coordinates of the sensor in relation to the welding seam. The seam tracker is integrated with the parallel robot (see Fig.9). During the seam tracking, five laser stripes are projected in the leading position, meanwhile the CCD camera observes the stripes and sends image data to the Scout controller that analyses the data and offers the local coordinate of camera related to the joint to the robot. In the robot controller a trajectory planning program has been designed to handle the data from Scout and correct the welding trajectory and an on-line teaching algorithm has been developed.

In the testing, the laser welding head is mounted on the robot end, and the Scout sensor is mounted in the front of welding head to lead the robot welding. The work piece is put randomly in y and z directions, and about 1 degree along Y and Z-axis, which are unknown for the robot before the seam finding. The maximum output power 3 kW YAG is used in the testing, which has 200mm focal length resulting a $\phi$0.6 mm focal spot on the work piece. The beam parameter product is 25 mm-mrad. The work piece is stainless steel AISI 316LN with 7mm thick , 600mm long, and 0.2 mm root gap for welding. Fig.9 shows the results of laser wilding with seam tracker.

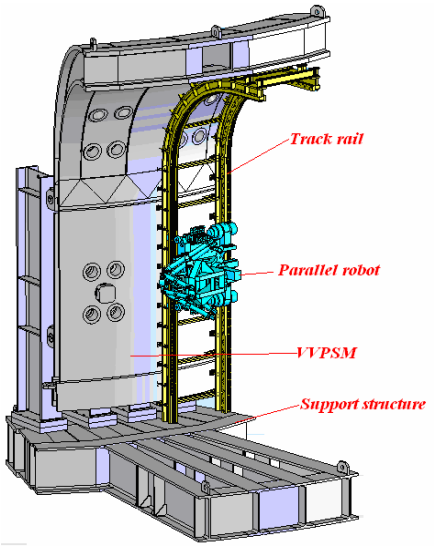


Figure 8. VVPSM mock-up

The machine cutting test was also carried out with stainless steel. The high speed steel cutting tool was used. It has 200mm diameter and 4mm thickness. The carbide tools are much more capable for cutting stainless steel and they are going to be used in the cutting operations to be performed in ITER.

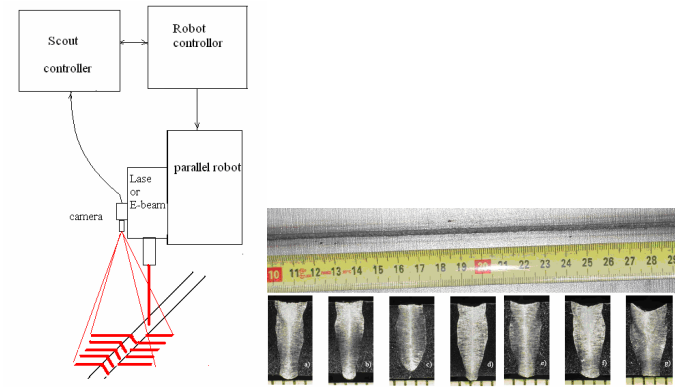


Figure 9. Laser welding test and Micrographs

## VI. MACHINING AND WELDING TEST MOCK-UP

The parallel robot is capable of holding all necessary machining tools and welding end-effectors in all positions accurately and stably. The kinematic analysis of the robot is presented. The models appeared to be complex, because of the redundant structure of the robot. The models had to be derived separately for Hexa-WH and the carriage mechanism. An optimization algorithm ensuring the maximum stiffness during the robot motion is employed in the trajectory planning. The experimental results of laser welding tests with seam tracker are shown. The results were obtained by a commercially available 6-DOF seam tracker and specially designed on-line teaching algorithms. The results demonstrate the applicability of the proposed solutions quite well.

## ACKNOWLEDGMENT

The laser welding test was carried out in collaboration with laser laboratory of VTT in Lappeenranta, Finland, and the whole work, supported by the European communities under the contract of Association between EURATOM/Finnish TEKES, was carried out within the framework of the European Fusion Development Agreement, The views and opinions expressed herein do not necessarily reflect those of the European Commission.

## REFERENCE

[1] D. Stewart, A platform with six degree of freedom, Proc. Inst. Mech. Eng., London, Vol. 180, pp. 371-386, 1965

[2] Huapeng, Wu, Heikki Handroos, Pekka Pessi, Juha Kilkki, Lawrence Jones, “Development and control towards a parallel water hydraulic weld/cut robot for machining processes in ITER vacuum vessel”, Fusion Engineering and Design, 2005

[3] T. C. Arai, K. Homma, H. Adachi, and Nakamura, Development of parallel link manipulator for underground excavation task, Proc. Int. Symposium on Advanced Robot Technology, pp. 541-548. 1991.

[4] C. Gosselin and J. Hamel, The agile eye: A high-performance three degree of freedom camera –orienting device, Proc. IEEE Int. Conference on Robotics and Automation, pp. 781-786. 1994.

[5] L. W. Tsai, Robot analysis: The mechanics of serial and parallel manipulators, A Wiley-Interscience Publication, John Wiley & Sons Inc. 1999.